

A Novel Solar and Electromagnetic Energy Harvesting System With a 3-D Printed Package for Energy Efficient Internet-of-Things Wireless Sensors

Jo Bito (美藤 成), *Student Member, IEEE*, Ryan Bahr, *Student Member, IEEE*,
 Jimmy G. Hester, *Student Member, IEEE*, Syed Abdullah Nauroze, *Student Member, IEEE*,
 Apostolos Georgiadis, *Senior Member, IEEE*, and Manos M. Tentzeris, *Fellow, IEEE*

(Invited Paper)

Abstract—This paper discusses the design of a novel dual (solar + electromagnetic) energy harvesting powered communication system, which operates at 2.4 GHz ISM band, enabling the autonomous operation of a low power consumption power management circuit for a wireless sensor, while featuring a very good “cold start” capability. The proposed harvester consists of a dual port rectangular slot antenna, a 3-D printed package, a solar cell, an RF-dc converter, a power management unit (PMU), a microcontroller unit, and an RF transceiver. Each designed component was characterized through simulation and measurements. As a result, the antenna exhibited a performance satisfying the design goals in the frequency range of 2.4–2.5 GHz. Similarly, the designed miniaturized RF-dc conversion circuit generated a sufficient voltage and power to support the autonomous operation of the bq25504 PMU for RF input power levels as low as -12.6 and -15.6 dBm at the “cold start” and “hot start” condition, respectively. The experimental testing of the PMU utilizing the proposed hybrid energy harvester confirmed the reduction of the capacitor charging time by 40% and the reduction of the minimum required RF input power level by 50% compared with the one required for the individual RF and solar harvester under the room light irradiation condition of 334 lx.

Index Terms—Additive manufacturing, autonomous RF system, energy harvesting, hybrid system, Internet of Things (IoT), power management, radio frequency (RF) circuits, rectennas, solar cell, 3-D printing, wireless sensors.

I. INTRODUCTION

NOWADAYS, the desire for a smart society that utilizes technologies such as large-scale sensor networks [1], the Internet of Things (IoT) [2], and smart skins [3], [4]

Manuscript received October 16, 2016; revised January 5, 2017; accepted January 22, 2017. Date of publication February 15, 2017; date of current version May 4, 2017. The work of J. Bito, R. Bahr, J. G. Hester, S. A. Nauroze, and M. M. Tentzeris was supported in part by the National Science Foundation Emerging Frontiers in Research and Innovation, in part by the Defense Threat Reduction Agency, in part by the Semiconductor Research Corporation, and in part by Texas Instruments. The work of A. Georgiadis was supported by the EU H2020 Marie Skłodowska-Curie under Grant Agreement 661621.

J. Bito, R. Bahr, J. G. Hester, S. A. Nauroze, and M. M. Tentzeris are with the School of Electrical and Computer Engineering, Georgia Institute of Technology, Atlanta, GA 30332 USA (e-mail: jbito3@gatech.edu).

A. Georgiadis is with the Institute of Sensors, Signals and Systems, Heriot-Watt University, Edinburgh EH14 4AS, U.K. (e-mail: a.georgiadis@hw.ac.uk).

Color versions of one or more of the figures in this paper are available online at <http://ieeexplore.ieee.org>.

Digital Object Identifier 10.1109/TMTT.2017.2660487

is continuously growing. One of the most pressing issues is the lack of a sustainable power supply that could enable the autonomous operation of these sensors and devices (motes). Conventional autonomous devices heavily rely on primary batteries, which can power the devices for only a certain amount of time. Once the sensor devices use up the stored energy in their batteries, the batteries need a replacement at a cost that increases significantly as the number of sensor devices in the system increases. To avoid this maintenance cost issue and achieve completely self-sustainable low-cost ubiquitous systems for the IoT and smart cities, research communities have devoted a considerable interest in ambient energy harvesting technologies. To maintain an effective operation of truly autonomous systems, this technology set harnesses energy from numerous ambient power sources such as solar, heat, vibration, and electromagnetic waves using transducers and stores it in energy storage components such as secondary batteries and capacitors [5]–[7]. Among the ambient energy sources, radio frequency (RF) energy is a highly attractive energy source because of its almost ubiquitous availability, especially in urban areas as well as the low cost and size of transducers [8], [9]. However, compared to the energy density of other energy sources, that of RF energy is typically very low [5]. Therefore, RF energy harvesters cannot directly drive devices that require relatively high power and voltage such as microcontrollers, especially from a “cold start” condition. Since low energy density levels cause a low RF-dc conversion efficiency, RF energy harvesting is even more challenging to be practically exploited [10]–[12].

A. Additive Manufacturing Techniques for Ambient Energy Harvesting Modules

To overcome the low-energy-density problem in RF energy harvesting, researchers have strived in the last several decades to improve the performance of RF energy harvesters. In the process, additive manufacturing technology has emerged as an alternative to conventional fabrication techniques such as etching and milling [13]–[15]. Specifically, additive manufacturing technology including inkjet printing, 3-D printing, and screen

printing has proven to be a very efficient solution for low-cost RF circuit patterning associated with an inherently high 2-D/3-D resolution and a wide variety of printable materials [16]. In the field of electrical engineering, the inkjet-printing technology has already enabled the easy realization of high-resolution conductive traces that can support the operation of circuits up to the subterahertz frequency range on a variety of substrates including flexible materials such as paper, plastic, and liquid crystal polymer [17], [18]. In addition to conductive materials, various dielectric materials and semiconductive materials can be printed using inkjet-printing technology, which allows for the full printing of most basic circuit components such as capacitors, inductors, antennas, diodes, and so on [19]–[21]. Another additive manufacturing technique, which has recently attracted the attention of the research community, is 3-D printing, especially the fused deposition modeling (FDM) technology [22], [23]. The wide variety of printable materials for these additive manufacturing techniques has also enabled the easy fabrication of both transducers and energy storage components for ambient harvesting from most energy sources.

B. Multienergy Source Hybrid Energy Harvesting

Numerous renewable ambient energy sources, such as solar, heat, vibration, and electromagnetic waves, exist in nature. Each ambient energy source exhibits different characteristics, and they all have both advantages and disadvantages. In reality, when autonomous systems completely rely on ambient energy sources, the major challenges associated with harvesting a single source of energy can cause critical issues for device operation. For example, an autonomous system relying exclusively on the energy harvested by a photovoltaic panel (e.g., a solar panel) will fail in the absence of light. Instead of relying on a single source, energy harvesting of multiple sources can be complementary and enable truly autonomous operation, as mentioned in [5]. Among various ambient energy sources, solar energy has been one of the most commonly sought-after because of the large power density available for harvesting during the daytime (ca. 100 mW cm^{-2}). Niotaki *et al.* [24] have reported on a hybrid RF/solar energy harvester, which can significantly increase the total available power available in a system. As another example, Georgiadis and Collado [25] and Donno *et al.* [26] have demonstrated a hybrid solar/EM energy harvesting system which extends the operation range of a passive RFID tag. The power conversion efficiency of electromagnetic energy contained in the solar spectrum to electricity depends on the level of illumination, the photoactive material and device architecture used. At low irradiance levels, like the ones found indoors (ca. $100 \mu\text{W cm}^{-2}$), the performance of a photovoltaic device becomes limited by increased power losses that arise as the value of the device shunt resistance becomes comparable to that of the characteristic resistance of the cell; defined as the ratio between the open circuit voltage and the short-circuit current. Among current photovoltaic technologies, those based on organic semiconductors shown in [27] and [28] are particularly suitable for low-light level operation. In addition, organic photovoltaic devices are

compatible with all-additive manufacturing methods such as ink-jet printing [29] and are therefore attractive for integration with RF energy harvesting modules to increase the available power per unit area [30]–[32].

C. Challenges in Ambient RF Energy Harvesting

Regardless of the typically low energy density of ambient RF, RF energy harvesting is an attractive research topic for various reasons. First, RF energy can inherently penetrate most walls, even opaque walls, so it is potentially more widespread available than other ambient energy sources. In addition, RF energy harvesters can operate at any time of the day and with any topology. Finally, their miniaturized form factor, their small physical dimensions, and lightweight enable us to easily carry or wear them. On the other hand, the typically low ambient RF energy density can be highly problematic, especially when the RF energy harvester is integrated with entirely autonomous systems because of their minimum input power and voltage requirements. As a general trend, Schottky diodes have been mainly used for RF energy harvesting because of their low threshold voltage and fast switching speed. However, Hemour and Wu [33] have reported that the performance of off-the-shelf Schottky diodes are reaching the maximum theoretical RF-dc conversion efficiency because of inevitable series resistance, junction capacitance, and high junction resistance associated with their operation principle, especially with low RF input power. Therefore, several studies have recently applied special types of diodes such as the backward tunnel (Esaki) diodes and the metal-insulator-metal diodes to rectify extremely low RF input power of below $1 \mu\text{W}$ [33], [34]. Another strategy is to maximize the available RF input power using multiband frequencies by introducing an ultrawideband/ multiband antenna and a wideband matching circuit topology in the rectenna [8], [35]–[37].

Recently, subthreshold operation of a switching transistor has been studied actively and it has been proven that some transistors can operate even below 0.4 V in the field of research [38], [39]. However, most off-the-shelf circuit components require relatively high operation voltage. For example, a typical transistor gate-source voltage requires at least 0.5 V for switching operation and ICs such as microcontrollers require an even higher operation voltage above 1.5 V [12], [40], [41], whereas typical voltages from the rectifier with RF input power under -20 dBm are below 0.3 V [42]. To overcome this low-voltage issue, researchers have developed dc–dc converters with low input voltage operation capabilities. Carlson *et al.* [43] reported a dc–dc boost converter that generates the output voltage of 1 V from the input voltage as low as 20 mV , with the power consumption of $1.6 \mu\text{W}$. However, the voltage regulator requires at least 0.6 V of start up voltage in a capacitor to initially start the operation of the circuit oscillators. Another example is a self-powered dc–dc converter reported in [44], which can generate the output voltage of 1 V from an input voltage close to 100 mV without any external power supply, but it requires at least $10 \mu\text{W}$ of input dc power and reported dc–dc conversion efficiency is below 25% because of inevitable power loss

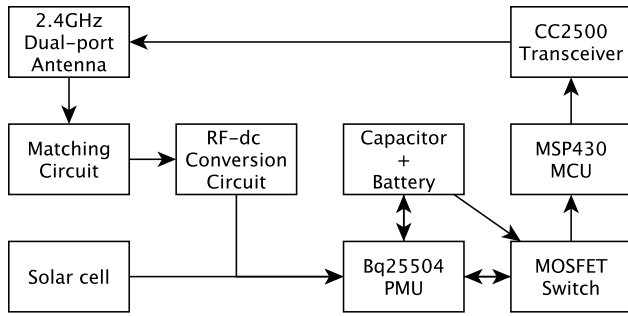


Fig. 1. Block diagram of a hybrid RF solar powered autonomous mote.

associated with the self-oscillation. To satisfy both of these power and voltage requirements, reported RF power sensitivity is -13 dBm for 1 V and -7 dBm for 3 V of output voltage. These facts imply that adding solar cells, which generate a nearly constant voltage under sufficient illumination conditions can enable the “cold start” start-up operation of a dc–dc converter allowing RF energy harvesters to then scavenge low power energy. At the same time, RF energy harvesters continuously generate energy during the night time when solar cells cannot generate any power.

To sufficiently address the main challenges of RF energy harvesting, by taking advantage of the unique features of additive manufacturing, one possible solution is the combination of multiple source ambient energy harvesting. In particular, this research proposes the hybridization of RF and solar energy harvesters in modules/topologies that can be fabricated utilizing additive manufacturing technology. The following sections of this paper deal with an overview of the proposed hybrid RF solar energy harvesting system, the design and preliminary measurements of the antenna and the rectifier, the preliminary module-level operation results and the hybrid harvester benchmarking in comparison to previously reported RF/solar energy harvesters, while this paper closes with the conclusions.

II. HYBRID RF SOLAR ENERGY HARVESTING SYSTEM

As a proof-of-concept prototype that can be easily implemented in a compact form factor, this research utilized a TI bq25504 ultralow power boost converter with battery management IC, which has a self-powered dc–dc converter for “cold start” operation and a high efficiency dc–dc converter with maximum power point tracking for “hot start” operation [45]. Fig. 1 shows the block diagram of an autonomous hybrid RF solar powered sensor device (mote). The device consists of a dual port antenna both for harvesting and communication at the 2.4 GHz ISM band, a solar cell, a matching circuit, an RF-dc conversion circuit, a bq25504 power management unit (PMU), a capacitor/battery for energy storage, a MOSFET switch, an MSP430 microcontroller unit (MCU) [41], and a CC2500 transceiver for communications [46].

III. ANTENNA DESIGN AND MEASUREMENT

This proposed system uses the 2.4 GHz ISM band for both energy harvesting and communications. Therefore, the

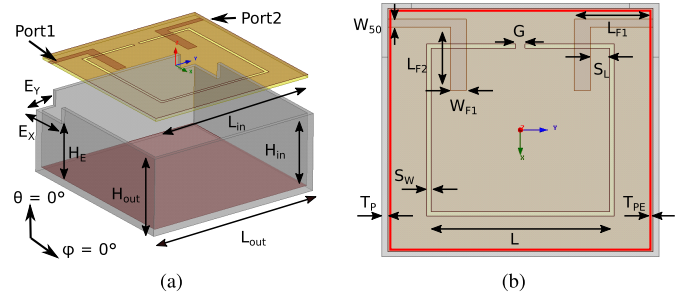


Fig. 2. (a) Side and (b) top views of the prototype of the rectangular shorted antenna.

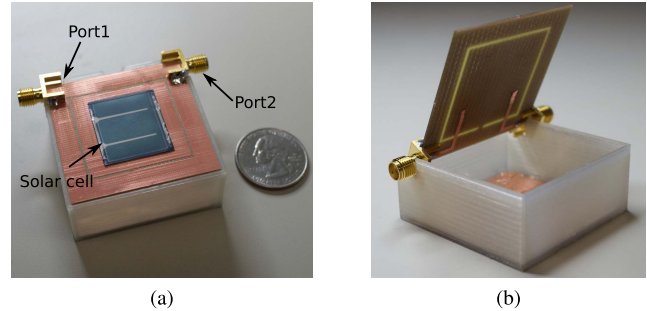


Fig. 3. Prototype of the dual-feed rectangular shorted slot solar antenna with a flexible film solar cell. (a) Top. (b) Inside.

antenna requires a dual port configuration with a high two-port isolation. In addition, circular polarization is suitable for RF energy harvesting as it allows the rectenna to capture signals with arbitrary linear polarization. In this scenario, a properly excited rectangular shorted slot antenna [47], [48] was identified as a strong candidate which also exhibits a good impedance and polarization bandwidth. The biggest novelty and challenge in designing the antenna for our energy harvesting capable mote is to feature a simultaneous two-port operation; one port for energy harvesting and another port for communication while sharing the same rectangular slot. The design and location of the feeding transmission lines as well as the size and height of the ground plane are critical to realize a good matching for both ports and a simultaneous high isolation between the two ports. Since the rectangular shorted slot antenna is an omnidirectional antenna, a reflector was placed on the bottom of the package in order to increase the gain. The package was printed utilizing a 3-D printer to precisely control the distance between the ground of the antenna and the reflector. The antenna was designed utilizing HFSS and fabricated on a 0.762 mm FR4 substrate with dielectric constant of 4.4 and loss tangent of 0.002 utilizing an LKPF ProtoMat S60 mechanical milling machine. Fig. 2 shows the side and top views of the rectangular shorted antenna and Table I summarizes the antenna design parameters. In this research, port1 is for harvesting and port2 is for communication. Fig. 3 shows the pictures of the prototype of the solar antenna, i.e., an antenna with an embedded solar cell. The package was created utilizing an FDM printer with polylactic acid (PLA)-based material. For an initial simulation, the dielectric constant of 3.1 and the loss tangent of 0.01 [49] were adopted. However, Meriakri *et al.* [50] have reported a wide variation of dielectric

TABLE I
PRELIMINARY DIMENSIONS OF THE DUAL-FED
RECTANGULAR SHORTED ANTENNA

Parameter	H_{in}	H_{out}	H_E	L_{in}	L_{out}	E_X	E_Y
Length (mm)	18	20	14	45	47	10	5
Parameter	L_{F1}	L_{F2}	L	W_{F1}	W_{50}	S_W	S_L
Length (mm)	13.35	7	11.81	31	1.46	0.9	3.1
Parameter	G	T_P	T_{PE}				
Length (mm)	1.6	1	0.5				

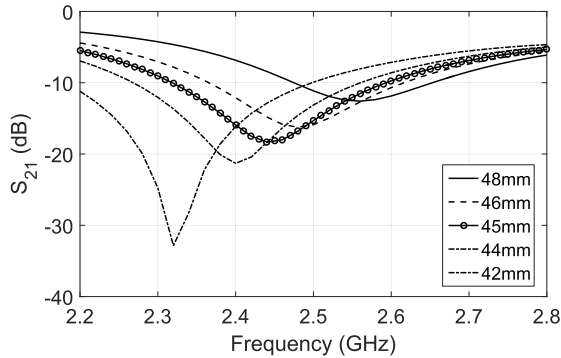
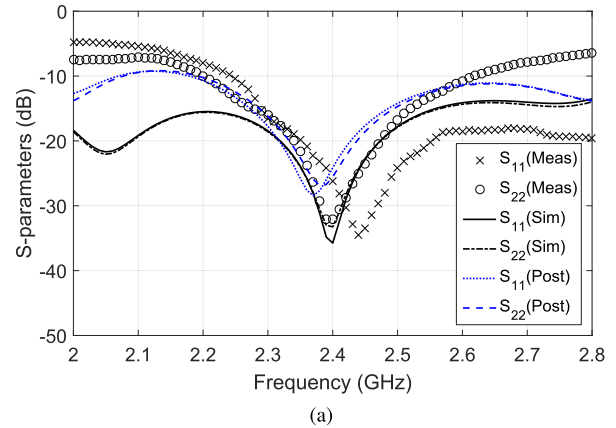


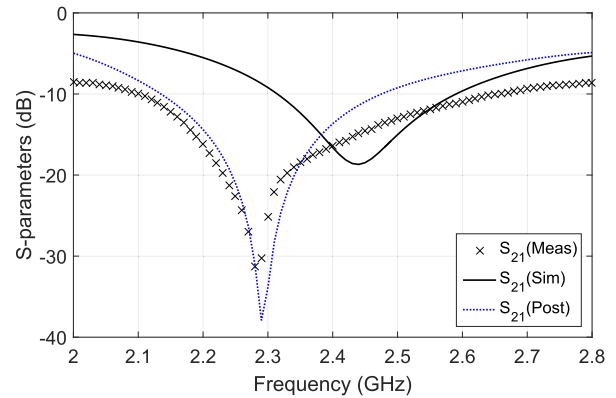
Fig. 4. Simulated S_{21} with respect to frequency with varied ground size.

constant of PLA material (2.76 to 15.7) which can cause a shift in the fabricated antenna operation frequency.

The design goals of the antenna are the following: 1) S_{11} and S_{22} below -13 dB (5%); 2) S_{21} below -13 dB (5%); and 3) axial ratio below 3 dB in the frequency range of 2.4–2.5 GHz. To satisfy these design goals, the length (L) of the sides of the square slot and the length of the gap (G) were determined to obtain a resonance at 2.45 GHz. In terms of impedance matching, the length and the width of the feeding signal lines can be adjusted to control the center frequency of operation. In addition, the proposed antenna design can adjust the center frequency of the two-port isolation (the peak of transmission loss) almost independently of the matching condition by varying the length of the square side of the ground plane (L_{in}). As illustrated in Fig. 4, preliminary simulations varied L_{in} from 42 to 48 mm, while a value of 45 mm was adopted for the initial antenna prototype. Fig. 5(a) depicts the simulated (design and post fabrication) and measured S_{11} and S_{22} , respectively. From the measurement, the antenna features the operation range of 2.28–2.55 GHz, and the simulation results match well with the measurement results. However, as depicted in Fig. 5(b), the frequency at the peak of transmission loss ($|S_{21}|$) was shifted to lower frequency. During the fabrication, an extra PLA layer with the thickness of 0.5 mm was added below the top printed circuit board (PCB) as a mechanical support of the antenna structure preventing the top PCB from dropping in the middle of the box. This extra thickness (T_{PE}) was taken into account in the postfabrication simulation model. Also, as mentioned above, the dielectric constant of the PLA material for the package can be higher than the value used in the initial simulation. Therefore, the postfabrication simulation adopted the dielectric constant of 4, and the simulation exhibited a good agreement with the measurement. This fact implies that further accurate



(a)



(b)

Fig. 5. Measured and simulated (design and postfabrication) (a) S_{11} , S_{22} , and (b) S_{21} of the dual-feed rectangular shorted slot antenna.

simulations for the antenna design require the accurate characterization of the 3-D printed PLA material. Over all, the measured S-parameters satisfied the design goals 1) and 2).

In addition to the S-parameters, this paper characterized the other properties of the antenna through simulations and measurements. Fig. 6(a) and (b) shows the simulated axial ratio with respect to frequency at broadside ($\theta = 0^\circ$) and θ direction rotation angle at 2.45 GHz, respectively. The axial ratio is about 3 dB in the frequency range of 2.4–2.5 GHz, which almost satisfies the design goal 3). Also, Fig. 7 which plots simulated total realized gain as a function of frequency yielding a value of 7.4 dB at the center frequency of 2.45 GHz. For the final prototype, a thin film solar cell, which Section IV explains the detail, is placed on top of the conductive area inside the slot without significantly disturbing its radiation characteristics. Therefore, the radiation patterns, depicted in Fig. 8, were also measured utilizing a LabVIEW controlled automatic rotation setup and a vector network analyzer (Anritsu 37369d). The measurement utilized a broadband horn antenna (AINFO LB-20245) as a reference. The measurements depicted in Fig. 8 show that the solar cell does not have a significant effect on the performance of the dual-feed rectangular antenna. Fig. 9 shows the side and the top view of the rectangular shorted antenna for the final prototype and Table II summarizes the final antenna design parameters. For simplicity in measurements, SMA connectors were connected

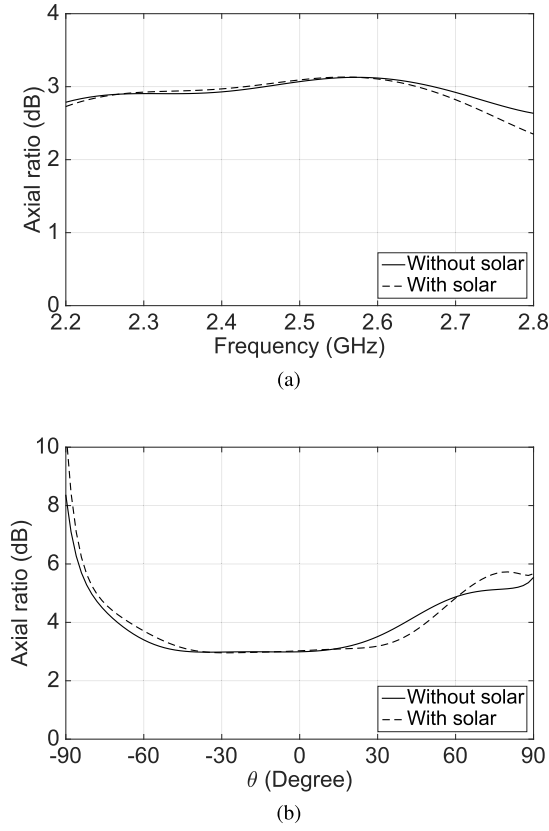


Fig. 6. Simulated axial ratio of the rectangular shorted antenna with and without the solar cell with respect to (a) frequency and (b) θ direction rotation angle.

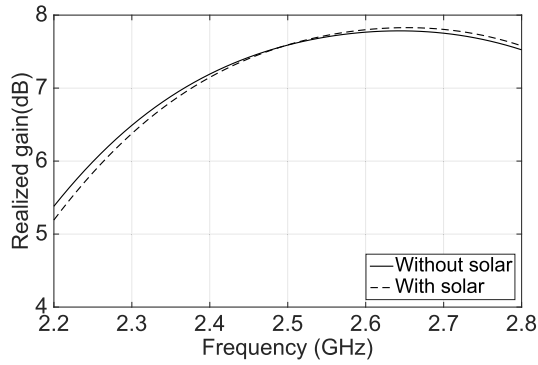


Fig. 7. Simulated total realized gain of the rectangular shorted antenna with and without the solar cell.

to the edges of the antenna, but the final prototype of the sensor device (mote) was designed to have all electronics connected to the antenna on the bottom layer near the center of the rectangular slot. Therefore, as shown in Fig. 9, the design of the excitation lines was modified for the final prototype. Fig. 10 shows the simulated S-parameters of the final antenna design.

IV. RF-DC CONVERSION CIRCUIT DESIGN AND MEASUREMENT

The solar cell selected for the proof-of-concept prototype was the Power Film MP3-25 solar cell which has the dimensions of 114 mm \times 24 mm, short circuit current $I_{sc} = 48$ mA,

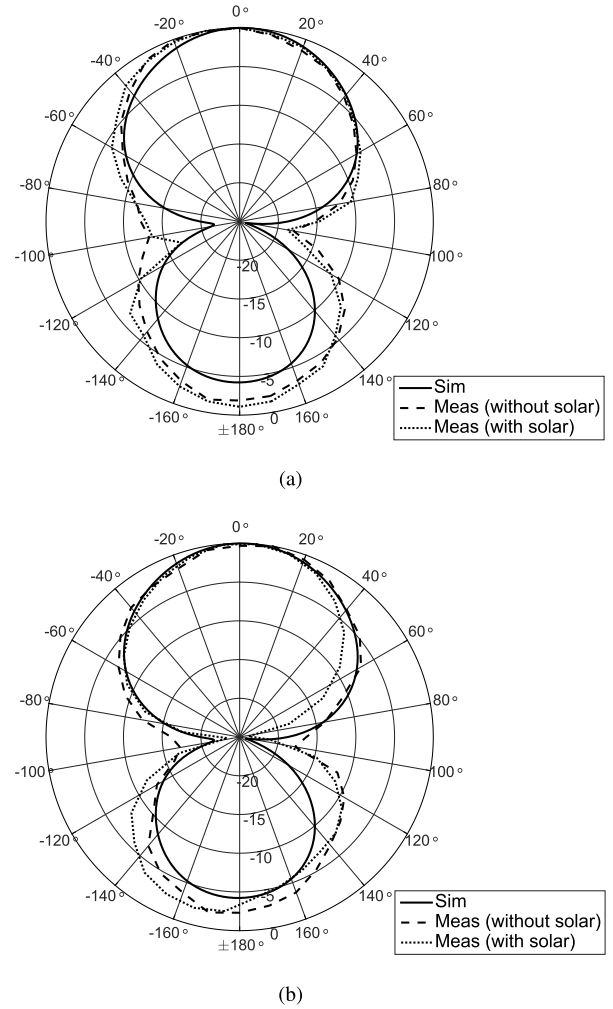


Fig. 8. Measured and simulated normalized radiation pattern of the rectangular shorted antenna with and without the solar cell. (a) $\phi = 0^\circ$. (b) $\phi = 90^\circ$.

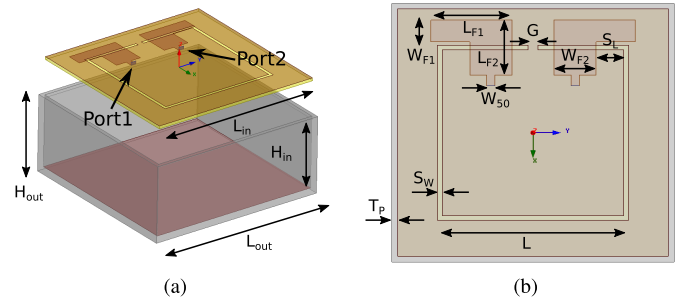


Fig. 9. (a) Side and (b) top views of the rectangular shorted antenna for the final prototype.

TABLE II
DIMENSION OF THE RECTANGULAR SHORTED ANTENNA FOR THE FINAL PROTOTYPE

Parameter	H_{in}	H_{out}	L_{in}	L_{out}	L_{F1}	L_{F2}	L
Length (mm)	18	20	45	47	13.5	10	31
Parameter	W_{F1}	W_{F2}	W_{50}	S_W	S_L	T_P	G
Length (mm)	4	7	1.46	0.9	4.6	1	1.6

open circuit voltage $V_{oc} = 4.1$ V, and can provide up to 93 mW at 3 V under 1 sun irradiance of 100 mW cm⁻². Specifically for the 3-D printed prototype discussed in this paper, only one fifth of the length of the solar module,

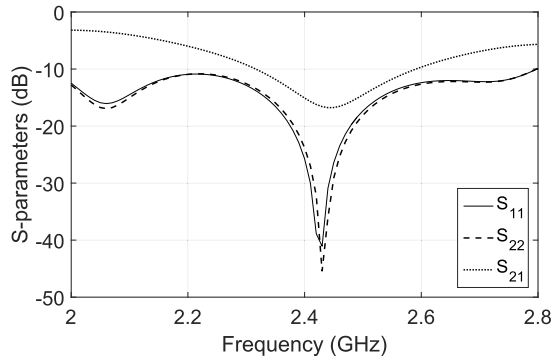


Fig. 10. Simulated S-parameters of the final antenna design with respect to frequency.

which exhibits about 0.68 V of open voltage and about 70.5 μW of maximum power under a room light condition ($334 \text{ lx} = 49 \mu\text{W} \cdot \text{cm}^{-2}$) with a dc load resistance of 3.8 k Ω , was utilized in order to fit within the conductive surface inside the dual-fed slot antenna, as shown in Fig. 3(a). The equivalent circuit model of the solar cell was utilized to design the harvester circuit in ADS. To begin with, this paper initially characterized the RF-dc conversion circuit independent of the solar cell.

The goal of the RF-dc conversion circuit design was to produce sufficient voltage and power to drive the PMU. Specifically, the bq25504 IC requires 330 mV and 15 μW to start up from a “cold state,” and it can sustain operation for a minimum input voltage of 80 mV. Also, the IC has an integrated maximum power point tracking function which optimally adjusts the load resistance value for the maximum output power [45]. This paper utilized a two diode RF rectifier (voltage doubler) circuit, which was necessary to accommodate a sufficiently high voltage to facilitate the start-up of the dc-dc converter circuit, as shown in Fig. 11(a). To simplify the layout, the solar cell output was connected using a series diode at the output of the RF rectifier circuit as depicted in Fig. 11.

The matching circuit design was optimized to maximize the dc output power for a given RF available input power of -17 dBm . This is the minimum required RF input power to generate the minimum dc input voltage (80 mV) of the PMU in the “hot state,” according to preliminary simulations for different dc output current values from the solar cell, corresponding to different solar light irradiation conditions. Figs. 12 and 13 show the RF-dc conversion efficiency and the output voltage of the rectifier prototype without connecting a solar cell as a function of the frequency for an input RF power level of -17 dBm and as a function of the power level of the input (harvested) RF signals at the frequency of 2.45 GHz, respectively. In these figures, both “ideal” and “nonideal” are simulation results with ADS. “Ideal” simulations use ideal lumped component models and “nonideal” simulations use nonideal lumped component models, provided by Johanson Technology for the components used in the prototype. For these measurements, RF power was measured using an RF power meter (NRP-Z211 from Rohde and Schwarz). The aggregate dc output power (P_{out}) from the RF energy harvester and the solar cell was calculated using (1),

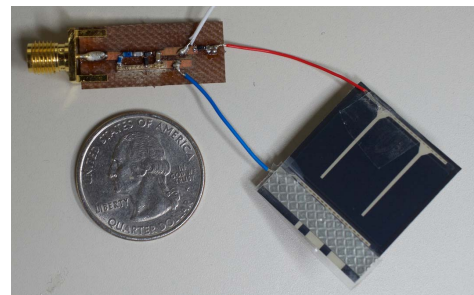
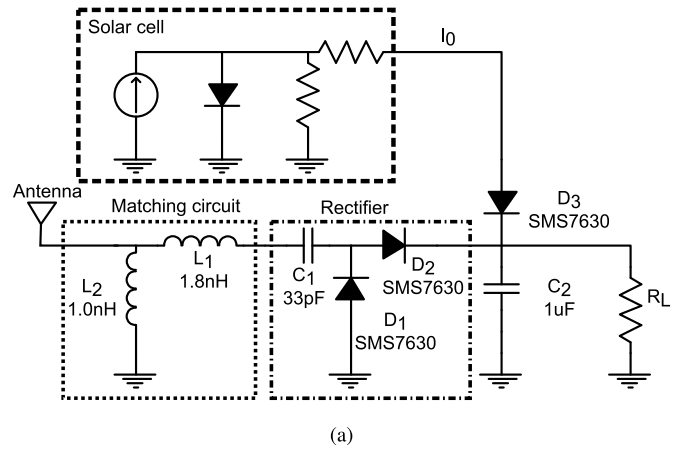


Fig. 11. (a) Circuit diagram of the hybrid RF solar harvester. (b) Photograph of the complete harvester prototype.

where V_{out} is the measured output voltage and R_{load} is the load resistance. The RF energy harvester exhibits about 20%–45% RF-dc conversion efficiency depending on the RF input power in the range of -17 – 0 dBm

$$P_{\text{out}} = \frac{V_{\text{out}}^2}{R_{\text{load}}}. \quad (1)$$

Next, the performance of the RF-dc conversion circuit including the solar cell was characterized through simulations and measurements. Fig. 14(a) and (b) depicts the output power and the output current from the solar cell for the optimal load resistance of 3.8 k Ω with reference to the ambient light intensity, respectively. The light intensity, measured utilizing a luminometer, was controlled by adjusting the distance between a table lamp and the solar cell. From these measurements, the solar cell yielded 70.5 μW of output dc power and 135.5 μA of output dc current at the room light condition of 334 lx irradiation. In addition, this paper simulated the output power from the hybrid RF solar harvester with respect to the current from the solar cell (I_0) for the RF power levels of -17 and -10 dBm for the optimal load at 2.45 GHz as shown in Fig. 15. The simulation results confirm that the dc combination of the solar cell and the RF circuit exhibits a higher output dc power without affecting the performance of the RF-dc conversion circuit and the solar cell. However, if the solar energy is dominant, the performance of the solar

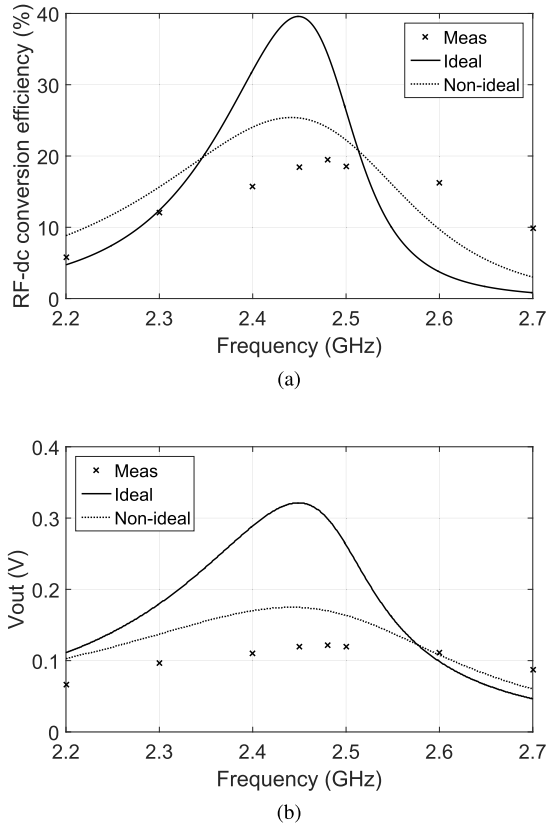


Fig. 12. Measured and simulated (a) RF-dc conversion efficiency and (b) dc output voltage with respect to frequency with optimal load resistance at -17 dBm RF input power.

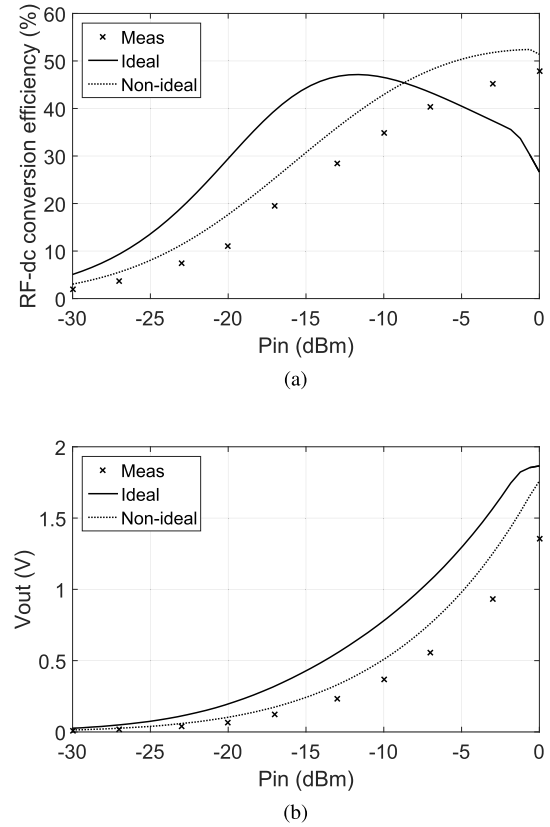


Fig. 13. Measured and simulated (a) RF-dc conversion efficiency and (b) dc output voltage with respect to input power with optimal load resistance at 2.45 GHz.

cell slightly degrades. Finally, Fig. 16 shows the simulated and the measured S_{11} of the harvester for the input RF power of -17 dBm at 2.45 GHz when the input current from the solar cell is varied. The current from the solar cell was varied by changing the light intensity in the same manner as described above. The return loss ($|S_{11}|$) increases first as I_0 increases, but it decreases if the input current is too large and the solar power is dominant.

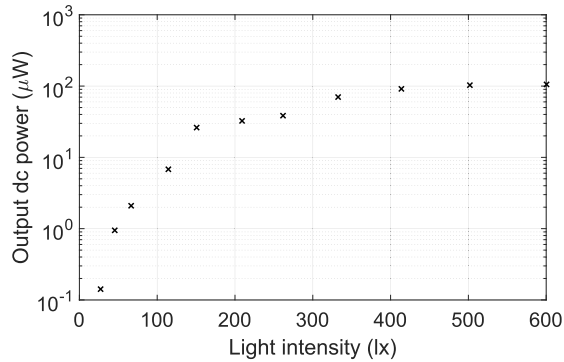
V. MODULE-LEVEL OPERATION TEST

After optimizing the subsystems of the proposed hybrid harvester, a module-level operation test of the RF solar harvester utilizing a bq25504 module as a load resistance R_L in Fig. 11(a) was performed to evaluate the capability of the harvester to “cold” start up the PMU. Fig. 17 shows the voltage of the $100 \mu\text{F}$ capacitor that is integrated in the bq25504 PMU during charging. The dashed line expresses the threshold of 1.5 V when the IC switches the operation mode from the cold start to the hot start. Similarly, the dotted line indicates the threshold of 2.8 V when VBAT_OK signal, which is a digital output for a battery good indicator, from the PMU is sufficiently high so that the capacitor voltage is adequate and the energy storage capacitor is ready to power the external dc load by turning on a MOSFET switch. The maximum output voltage is regulated at 3.3 V to protect a battery which can be externally connected, but this voltage can be arbitrary selected within the range of 2.4 – 5.3 V. The first three traces in Fig. 17

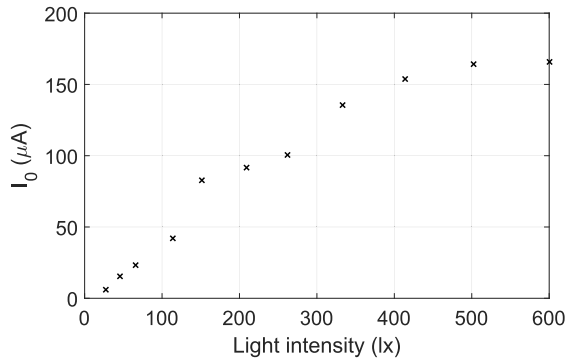
represent three different charging conditions: 1) -12.6 dBm RF input power; 2) solar cell at room light condition; and 3) aggregate dc combining the two harvesters, respectively. The input RF power of -12.6 dBm is the minimum required RF power to start the operation of bq25504 module from the “cold start” condition without using any solar cell. The comparison between 2) and 3) in Fig. 17 suggests that the charging time significantly decreases combining the dc output of the solar and the RF harvesters. More specifically, the time to charge the capacitor from 0 to 2.8 V under the charging conditions 2) and 3) is 86 and 51 s, respectively. Therefore, 40% of capacitor charging time reduction is confirmed through the measurement. The last trace in Fig. 17 shows another charging condition 4) by combining the dc outputs of the solar and the RF harvester for the lower input power level of -15.6 dBm. In this trace, the change in slope around 2.5 V indicates that the light intensity was drastically reduced from 334 to 18.9 lx at this point by covering the solar cell. The input RF power of -15.6 dBm, which is the half of -12.6 dBm, cannot support alone the operation of the “cold start” operation mode. However, with the help of solar energy, this hybrid energy harvesting system can go over the “cold start” mode. For nonsufficient light irradiation conditions (e.g., in the night or in completely dark rooms), even a solar panel may not be used to “cold start” the system. However, once the IC starts operating with “hot start” mode after an initial relatively strong light irradiation, the input RF power of -15.6 dBm can

TABLE III
ENERGY HARVESTING SYSTEM PERFORMANCE COMPARISON

	Energy source	Antenna frequency	Maximum gain (dBi)	Polarization	Communication capability	Load	Sensitivity
This work	EM/Light	2.28 to 2.55 GHz	7.4	Circular	RF Transceiver (simultaneously with harvesting)	PMU (bq25504) MCU RF Transceiver Sensor	-15.6 dBm @ 2.8 V
Niotaki [24]	EM/Light	2.3 to 2.45 GHz	1.9	-	-	PMU (bq25504) Sensor (Simulation)	-
Georgiadis [25]	EM/Light	868 MHz (no measurement data)	-	Linear	RFID	Oscillator	9.3 dBm @1.7V
De Donno [26]	EM/Light	855 to 880 MHz	1.85	Linear	-	MCU Dc-dc converter Sensor EEPROM	-14 dBm @ 2.4 V
Pinuela [9]	EM	470 to 2017 MHz (multiple antennas)	4.48 to 4.76	Linear	-	PMU (bq25504)	-25 dBm (single) -29 dBm (array) @ 2.4 to 5.3 V
Vyas [8]	EM	511 to 566 MHz (wideband)	7.3	Linear	-	MCU Sensor	-14.6 dBm @ 1.8 V



(a)



(b)

Fig. 14. Measured (a) output dc power and (b) dc current (I_0) from the solar cell with respect to the light intensity for the load resistance of 3.8 k Ω .

maintain the perpetual operation of the IC, while the PMU gradually charges the capacitor using the ambient RF energy even under dark conditions.

VI. HYBRID HARVESTER SYSTEM PERFORMANCE BENCHMARKING

Recently, there have been various reported energy harvesting systems which utilize a PMU including a dc-dc

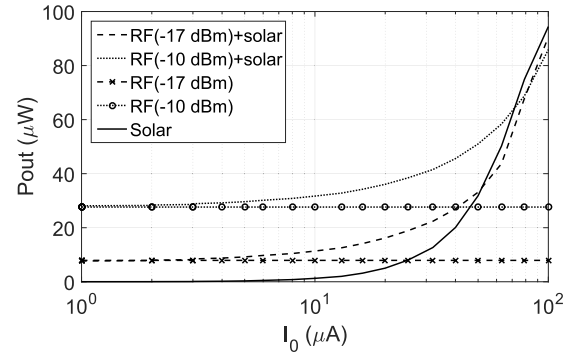


Fig. 15. Simulated output dc power with respect to the output dc current from the solar cell (I_0) for RF input power of -17 and -10 dBm.

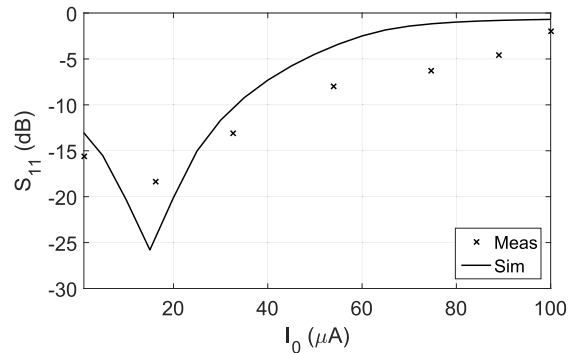


Fig. 16. Simulated and measured S_{11} with respect to output current from the solar cell (I_0).

converter to increase the sensitivity of the systems. Therefore, Table III summarizes the performance of recently reported EM/solar and EM energy harvesting system in terms of energy source, antenna operation frequency, maximum gain, antenna polarization, communication capability, dc load, and sensitivity, which is the minimum required RF power to satisfy the dc voltage and power requirements for their

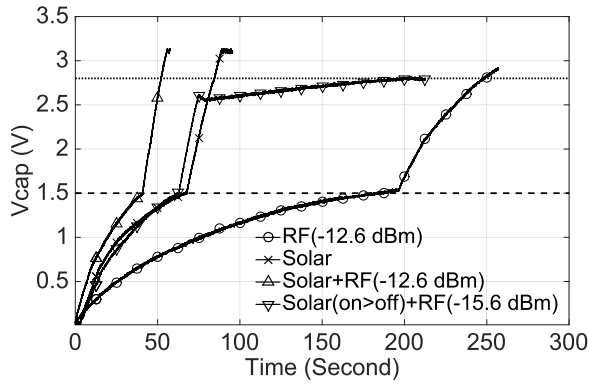


Fig. 17. Voltage in the $100 \mu\text{F}$ capacitor that is integrated in the bq25504 PMU during charging under different RF and solar conditions. (1) -12.6 dBm RF input power. (2) Solar under room light condition. (3) -12.6 dBm RF input power + solar under room light condition. (4) -15.6 dBm RF input power + solar under room light condition until cold start mode is over.

load. Compared with other EM/solar energy harvesters, the proposed design has the highest antenna operation bandwidth, highest gain, circular polarization, which is more suitable for ambient RF energy harvesting than linear polarization because of the unknown polarization of the harvested transmitting antennas, and simultaneous wireless communication capability while harvesting ambient energy. Regarding sensitivity, this paper exhibits the lowest required RF input power among the EM/solar energy harvesters summarized in Table III. The sensitivity can be increased by improving the RF-dc conversion efficiency and further reducing the system power requirement. For example, Pinuela *et al.* [9] have reported the lowest required RF input power of -29 dBm for the same bq25504 PMU for the cold-start. Although, according to the datasheet of bq25504 PMU, this IC requires the minimum dc input power of $15 \mu\text{W}$ for cold-start [45], which is more than 10 times higher than the reported sensitivity in [9] without considering RF-dc conversion loss that is typically more than 70% of RF input power with input power below -20 dBm.

VII. CONCLUSION

This paper investigates the potential of multiple energy harvesting system for the cold start and the subsequent perpetual operation of low profile the low power wireless sensor nodes. This research effort demonstrated the design of a dual solar and electromagnetic energy harvesting and communication system which operates at 2.4 GHz ISM band enabling the operation of a low power PMU for a wireless sensor. The harvester consists of a dual-port rectangular slot antenna, a 3-D printed package, a solar cell, an RF-dc converter, a PMU, an MCU, and an RF transceiver and every component was designed and characterized through simulation and measurements. As a result, this novel antenna with simultaneous harvesting and communication capabilities exhibited a performance satisfying the design goals of: 1) S_{11} and S_{22} below -13 dB; 2) S_{21} below -13 dB; and 3) axial ratio below 3 dB in the frequency range of

2.4–2.5 GHz. Similarly, the designed miniaturized RF-dc conversion circuit generated sufficient voltage and power to support the operation of the bq25504 PMU from RF input power as low as -12.6 and -15.6 dBm at the “cold start” and “hot start” condition, respectively. The module-level operation test of the PMU utilizing the hybrid RF/solar energy harvester confirmed a 40% reduction in the capacitor charging time and a 50% reduction in the minimum required RF input power compared to the independent operation of the RF and the solar harvester under the room light irradiation condition of 334 lx. As a future work, all circuit components in Fig. 1 will be integrated to two PCBs, one for the antenna, communication, and rectification and another one for the power management and the microcontroller. Both of them are arranged in a printed 3-D package which will have an opening to connect the MCU to a debugger to program the chip. We plan to connect the PCBs with a flexible ribbon cable in the package. The solar cell will be attached on the top of the communication/harvesting board. The MCU can be programmed for wireless measurement as reported in [15]. The proposed hybrid energy harvester could find numerous applications in IoT, smart skin and M2M applications in rugged operation conditions.

ACKNOWLEDGMENT

The authors would like to thank W. Chow, C. Fuentes-Hernandez, and B. Kippelen, all with the School of Electrical and Computer Engineering, Georgia Institute of Technology, for giving their precious advice about organic photovoltaic from the view point of their expertise.

REFERENCES

- [1] H. Nishimoto, Y. Kawahara, and T. Asami, “Prototype implementation of ambient RF energy harvesting wireless sensor networks,” in *Proc. IEEE SENSORS*, Nov. 2010, pp. 1282–1287. [Online]. Available: <http://dx.doi.org/10.1109/ICSENS.2010.5690588>
- [2] L. Atzori, A. Iera, and G. Morabito, “The Internet of Things: A survey,” *Comput. Netw.*, vol. 54, no. 15, pp. 2787–2805, Oct. 2010. [Online]. Available: <http://dx.doi.org/10.1016/j.comnet.2010.05.010>
- [3] L. Gao *et al.*, “Epidermal photonic devices for quantitative imaging of temperature and thermal transport characteristics of the skin,” *Nature Commun.*, vol. 5, p. 4938, Sep. 2014. [Online]. Available: <http://dx.doi.org/10.1038/ncomms5938>
- [4] B. S. Cook, T. Le, S. Palacios, A. Traille, and M. M. Tentzeris, “Only skin deep: Inkjet-printed zero-power sensors for large-scale RFID-integrated smart skins,” *IEEE Microw. Mag.*, vol. 14, no. 3, pp. 103–114, Mar. 2013. [Online]. Available: <http://dx.doi.org/10.1109/MMM.2013.2240855>
- [5] S. Kim *et al.*, “Ambient RF energy-harvesting technologies for self-sustainable standalone wireless sensor platforms,” *Proc. IEEE*, vol. 102, no. 11, pp. 1649–1666, Nov. 2014.
- [6] S. Priya and D. J. Inman, Eds., *Energy Harvesting Technologies*, vol. 21. New York, NY, USA: Springer, 2009.
- [7] J. A. Paradiso and T. Starmer, “Energy scavenging for mobile and wireless electronics,” *IEEE Pervasive Comput.*, vol. 4, no. 1, pp. 18–27, Jan./Mar. 2005.
- [8] R. J. Vyas, B. B. Cook, Y. Kawahara, and M. M. Tentzeris, “E-WEHP: A batteryless embedded sensor-platform wirelessly powered from ambient digital-TV signals,” *IEEE Trans. Microw. Theory Techn.*, vol. 61, no. 6, pp. 2491–2505, Jun. 2013.
- [9] M. Pinuela, P. D. Mitcheson, and S. Lucyszyn, “Ambient RF energy harvesting in urban and semi-urban environments,” *IEEE Trans. Microw. Theory Techn.*, vol. 61, no. 7, pp. 2715–2726, Jul. 2013.

- [10] C. R. Valenta and G. D. Durgin, "Harvesting wireless power: Survey of energy-harvester conversion efficiency in far-field, wireless power transfer systems," *IEEE Microw. Mag.*, vol. 15, no. 4, pp. 108–120, Jun. 2014.
- [11] X. Lu, P. Wang, D. Niyato, D. I. Kim, and Z. Han, "Wireless networks with RF energy harvesting: A contemporary survey," *IEEE Commun. Surveys Tuts.*, vol. 17, no. 2, pp. 757–789, 2nd Quart., 2015.
- [12] K. Gudan, S. Shao, J. J. Hull, A. Hoang, J. Ensworth, and M. S. Reynolds, "Ultra-low power autonomous 2.4GHz RF energy harvesting and storage system," in *Proc. IEEE Int. Conf. RFID-TA*, Tokyo, Japan, Sep. 2015, pp. 176–181.
- [13] W. S. Wong, M. L. Chabinye, T.-N. Ng, and A. Salleo, "Materials and novel patterning methods for flexible electronics," in *Flexible Electronics* (Electronic Materials: Science & Technology). New York, NY, USA: Springer, 2009, pp. 143–181.
- [14] L. Yang, A. Rida, R. Vyas, and M. M. Tentzeris, "RFID tag and RF structures on a paper substrate using inkjet-printing technology," *IEEE Trans. Microw. Theory Techn.*, vol. 55, no. 12, pp. 2894–2901, Dec. 2007.
- [15] J. Bitto, J. G. Hester, and M. M. Tentzeris, "Ambient RF energy harvesting from a two-way talk radio for flexible wearable wireless sensor devices utilizing inkjet printing technologies," *IEEE Trans. Microw. Theory Techn.*, vol. 63, no. 12, pp. 4533–4543, Dec. 2015.
- [16] J. G. Hester *et al.*, "Additively manufactured nanotechnology and origami-enabled flexible microwave electronics," *Proc. IEEE*, vol. 103, no. 4, pp. 583–606, Apr. 2015.
- [17] B. Tehrani, B. Cook, J. Cooper, and M. Tentzeris, "Inkjet printing of a wideband, high gain mm-wave Vivaldi antenna on a flexible organic substrate," in *Proc. IEEE Antennas Propag. Soc. Int. Symp.*, Memphis, TN, USA, Jul. 2014, pp. 320–321.
- [18] J. Bitto, B. Tehrani, B. Cook, and M. Tentzeris, "Fully inkjet-printed multilayer microstrip patch antenna for Ku-band applications," in *Proc. IEEE Antennas Propag. Soc. Int. Symp.*, Memphis, TN, USA, Jul. 2014, pp. 854–855.
- [19] B. S. Cook, J. R. Cooper, and M. M. Tentzeris, "Multi-layer RF capacitors on flexible substrates utilizing inkjet printed dielectric polymers," *IEEE Microw. Wireless Compon. Lett.*, vol. 23, no. 7, pp. 353–355, Jul. 2013.
- [20] B. S. Cook *et al.*, "Inkjet-printed, vertically-integrated, high-performance inductors and transformers on flexible LCP substrate," in *IEEE MTT-S Int. Microw. Symp. Dig.*, Tampa, FL, USA, Jun. 2014, pp. 1–4.
- [21] N. Sani *et al.*, "All-printed diode operating at 1.6 GHz," *Proc. Nat. Acad. Sci. USA*, vol. 111, no. 33, pp. 11943–11948, 2014.
- [22] P. I. Deffenbaugh, R. C. Rumpf, and K. H. Church, "Broadband microwave frequency characterization of 3-D printed materials," *IEEE Trans. Compon., Packag. Manuf. Technol.*, vol. 3, no. 12, pp. 2147–2155, Dec. 2013. [Online]. Available: <http://dx.doi.org/10.1109/TCPM.2013.2273306>
- [23] S. Zhang, C. C. Njoku, W. G. Whittow, and J. C. Vardaxoglou, "Novel 3D printed synthetic dielectric substrates," *Microw. Opt. Technol. Lett.*, vol. 57, no. 10, pp. 2344–2346, Oct. 2015. [Online]. Available: <http://dx.doi.org/10.1002/mop.29324>
- [24] K. Niotaki, F. Giuppi, A. Georgiadis, and A. Collado, "Solar/EM energy harvester for autonomous operation of a monitoring sensor platform," *Wireless Power Transf.*, vol. 1, no. 1, pp. 44–50, Mar. 2014.
- [25] A. Georgiadis and A. Collado, "Improving range of passive RFID tags utilizing energy harvesting and high efficiency class-E oscillators," in *Proc. 6th Eur. Conf. Antennas Propag. (EuCAP)*, Mar. 2012, pp. 3455–3458. [Online]. Available: <http://dx.doi.org/10.1109/EuCAP.2012.6206429>
- [26] D. De Donno, L. Catarinucci, and L. Tarricone, "An UHF RFID energy-harvesting system enhanced by a DC-DC charge pump in silicon-on-insulator technology," *IEEE Microw. Wireless Compon. Lett.*, vol. 23, no. 6, pp. 315–317, Jun. 2013. [Online]. Available: <http://dx.doi.org/10.1109/LMWC.2013.2258002>
- [27] Y. Zhou, T. M. Khan, J. W. Shim, A. Dindar, C. Fuentes-Hernandez, and B. Kippelen, "All-plastic solar cells with a high photovoltaic dynamic range," *J. Mater. Chem. A*, vol. 2, no. 10, pp. 3492–3497, 2014.
- [28] J. Tong *et al.*, "Flexible all-solution-processed all-plastic multijunction solar cells for powering electronic devices," *Mater. Horizons*, vol. 3, no. 5, pp. 452–459, 2016.
- [29] T. M. Eggenhuisen *et al.*, "High efficiency, fully inkjet printed organic solar cells with freedom of design," *J. Mater. Chem. A*, vol. 3, no. 14, pp. 7255–7262, 2015.
- [30] M. Danesh and J. R. Long, "Photovoltaic antennas for autonomous wireless systems," *IEEE Trans. Circuits Syst. II, Exp. Briefs*, vol. 58, no. 12, pp. 807–811, Dec. 2011.
- [31] A. Collado and A. Georgiadis, "Conformal hybrid solar and electromagnetic (EM) energy harvesting rectenna," *IEEE Trans. Circuits Syst. I, Reg. Papers*, vol. 60, no. 8, pp. 2225–2234, Aug. 2013.
- [32] K. Niotaki, A. Georgiadis, and A. Collado, "Dual-band rectifier based on resistance compression networks," in *IEEE MTT-S Int. Microw. Symp. Dig.*, Tampa, FL, USA, Jun. 2014, pp. 1–3.
- [33] S. Hemour and K. Wu, "Radio-frequency rectifier for electromagnetic energy harvesting: Development path and future outlook," *Proc. IEEE*, vol. 102, no. 11, pp. 1667–1691, Nov. 2014.
- [34] C. H. P. Lorenz *et al.*, "Overcoming the efficiency limitation of low microwave power harvesting with backward tunnel diodes," in *IEEE MTT-S Int. Microw. Symp. Dig.*, Phoenix, AZ, USA, May 2015, pp. 1–4.
- [35] K. Niotaki, S. Kim, S. Jeong, A. Collado, A. Georgiadis, and M. M. Tentzeris, "A compact dual-band rectenna using slot-loaded dual band folded dipole antenna," *IEEE Antennas Wireless Propag. Lett.*, vol. 12, pp. 1634–1637, 2013. [Online]. Available: <http://dx.doi.org/10.1109/LAWP.2013.2294200>
- [36] H. Sun, Y.-X. Guo, M. He, and Z. Zhong, "A dual-band rectenna using broadband Yagi antenna array for ambient RF power harvesting," *IEEE Antennas Wireless Propag. Lett.*, vol. 12, pp. 918–921, 2013.
- [37] F. Bolos, D. Belo, and A. Georgiadis, "A UHF rectifier with one octave bandwidth based on a non-uniform transmission line," in *Proc. Inst. Elect. Electron. Eng. (IEEE)*, San Francisco, CA, USA, May 2016, pp. 1–3. [Online]. Available: <http://dx.doi.org/10.1109/MWSYM.2016.7540083>
- [38] A. Wang, B. H. Calhoun, and A. P. Chandrakasan, *Sub-Threshold Design for Ultra Low-Power Systems*, vol. 95. New York, NY, USA: Springer, 2006.
- [39] A. Bryant, J. Brown, P. Cottrell, M. Ketchen, J. Ellis-Monaghan, and E. J. Nowak, "Low-power CMOS at $V_{dd}=4kT/q$," in *Proc. Device Res. Conf.*, Jun. 2001, pp. 22–23. [Online]. Available: <http://dx.doi.org/10.1109/DRC.2001.937856>
- [40] M. A. M. Vieira, C. N. Coelho, D. da Silva, and J. da Mata, "Survey on wireless sensor network devices," in *Proc. IEEE Conf. Emerg. Technol. Factory Autom.*, Sep. 2003, pp. 537–544. [Online]. Available: <http://dx.doi.org/10.1109/ETFA.2003.1247753>
- [41] *MSP430F22x4: Mixed Signal Microcontroller*, Texas Instrum. Incorporated, Dallas, TX, USA, Aug. 2012.
- [42] K. Gudan, S. Shao, J. J. Hull, J. Ensworth, and M. S. Reynolds, "Ultra-low power 2.4GHz RF energy harvesting and storage system with -25dBm sensitivity," in *Proc. IEEE Int. Conf. RFID*, San Diego, CA, USA, Apr. 2015, pp. 40–46.
- [43] E. J. Carlson, K. Strunz, and B. P. Otis, "A 20 mV input boost converter with efficient digital control for thermoelectric energy harvesting," *IEEE J. Solid-State Circuits*, vol. 45, no. 4, pp. 741–750, Apr. 2010.
- [44] S.-E. Adami, V. Marian, N. Degrenne, C. Vollaie, B. Allard, and F. Costa, "Self-powered ultra-low power DC-DC converter for RF energy harvesting," in *Proc. IEEE FTFC*, Paris, France, Jun. 2012, pp. 1–4.
- [45] *BQ25504-Ultra Low Power Boost Converter With Battery Management for Energy Harvester Applications*, Texas Instrum. Incorporated, Dallas, TX, USA, Oct. 2012.
- [46] *CC2500: Low-Cost Low-Power 2.4 GHz RF Transceiver*, Texas Instrum. Incorporated, Dallas, TX, USA, 2010.
- [47] S. Shi, K. Hirasawa, and Z. N. Chen, "Circularly polarized rectangularly bent slot antennas backed by a rectangular cavity," *IEEE Trans. Antennas Propag.*, vol. 49, no. 11, pp. 1517–1524, Nov. 2001.
- [48] R. Li, B. Pan, A. N. Traillie, J. Papapolymerou, J. Laskar, and M. M. Tentzeris, "Development of a cavity-backed broadband circularly polarized slot/strip loop antenna with a simple feeding structure," *IEEE Trans. Antennas Propag.*, vol. 56, no. 2, pp. 312–318, Feb. 2008. [Online]. Available: <http://dx.doi.org/10.1109/TAP.2007.915412>
- [49] T. Nakatsuka, "Polylactic acid-coated cable," *Fujikura Tech. Rev.*, vol. 40, pp. 39–45, 2011.
- [50] V. V. Meriakri, D. S. Kalenov, M. P. Parkhomenko, S. Zhou, and N. A. Fedoseev, "Dielectric properties of biocompatible and biodegradable polycaprolone and polylactide and their nanocomposites in the millimeter wave band," *Amer. J. Mater. Sci.*, vol. 2, no. 6, pp. 171–175, Jan. 2013.



Jo Bito (S'13) received the B.S. degree in electrical and electronic engineering from Okayama University, Okayama, Japan, in 2013, and the M.S. degree in electrical and computer engineering from the Georgia Institute of Technology, Atlanta, GA, USA, in 2016, where he is currently pursuing the Ph.D. degree.

From 2010 to 2011, he joined the International Programs in Engineering at the University of Illinois at Urbana-Champaign, Champaign, IL, USA. He is currently a Research Assistant with the Agile Technologies for High-Performance Electromagnetic Novel Applications Group, Georgia Institute of Technology. His current research interests include the application of inkjet printing technology for flexible and wearable electronics, RF energy harvesting, and wireless power transfer systems.

Mr. Bito was a recipient of the Japan Student Services Organization Long Term Scholarship in 2013.



Syed Abdullah Nauroze (S'13) received the B.Sc. (Hons.) degree in computer engineering from the University of Engineering and Technology, Taxila, Pakistan, in 2005, and the M.Sc. degree in electrical engineering from the Royal Institute of Technology (KTH), Stockholm, Sweden, in 2008. He is currently pursuing the Ph.D. degree in electrical and computer engineering at the Georgia Institute of Technology, Atlanta, GA, USA.

From 2008 to 2009, he was with the Microsystems Technology Laboratory, KTH, where he was involved in on-chip millimeter-wave antennas for automotive radar and future wireless applications. He is currently a Research Assistant with the ATHENA Laboratory, Georgia Institute of Technology. He possesses seven years of teaching experience. His current research interests include application of additive manufacturing techniques such as 3-D printing and ink-jet printing for flexible and origami-based RF structures.

Mr. Nauroze was a recipient of the Swedish Institute Scholarship in 2006 and the Fulbright Scholarship in 2014 for his master's and Ph.D. degrees, respectively.



Ryan Bahr (S'11) received the B.S. and M.S. degrees in electrical engineering from the Georgia Institute of Technology, Atlanta, GA, USA, where he is currently pursuing the Ph.D. degree in electrical and computer engineering under the supervision of Prof. Tentzeris.

His current research interests include applying 3-D printing techniques for millimeter wave and packaging applications utilizing new materials.



Apostolos Georgiadis (S'94-M'02-SM'08) was born in Thessaloniki, Greece. He received the B.S. degree in physics and M.S. degree in telecommunications from the Aristotle University of Thessaloniki, Thessaloniki, in 1993 and 1996, respectively, and the Ph.D. degree in electrical engineering from the University of Massachusetts, Amherst, MA, USA, in 2002.

In 1995, he spent a semester with the Radio Antenna Communications, Milan, Italy, where he was involved with Yagi antennas for UHF applications. In 2000, he spent three months with Telaxis Communications, South Deerfield, MA, USA, where he was involved in the design and testing of a pillbox antenna for LMDS applications. In 2002, he joined the Global Communications Devices, North Andover, MA, USA, as a Systems Engineer, where he was involved in CMOS transceivers for wireless network applications. In 2003, he joined Bermat, Inc., Minnetonka, MN, USA, as an RF/Analog Systems Architect. In 2005, he joined the University of Cantabria, Santander, Spain, as a Juan de la Cierva Fellow Researcher. In 2006, he joined Bitwave Semiconductor, Lowell, MA, USA, as a Consultant. In addition, he collaborated with ACORDE S.A., Santander, where he was involved in the design of integrated CMOS voltage-controlled oscillators for ultrawideband applications. In 2007, he joined CTTC, Barcelona, Spain, as a Senior Researcher involved with communications subsystems, where he was a Group Leader with the Microwave Systems and Nanotechnology Department from 2013 to 2016. In 2016, he joined Heriot-Watt University, Edinburgh, U.K., as an Associate Professor. He has authored more than 150 papers in peer-reviewed journals and international conferences. His current research interests include energy harvesting and wireless power transmission, RFID technology, active antennas and phased array antennas, inkjet and 3-D printed electronics, and millimeter-wave systems.

Dr. Georgiadis is a member of the IEEE MTT-S TC-24 RFID Technologies (past Chair) and the IEEE MTT-S TC-26 Wireless Energy Transfer and Conversion. He is the EU Marie Curie Global Fellow. He received the Fulbright Scholarship for graduate studies at the University of Massachusetts in 1996, the Outstanding Teaching Assistant Award from the University of Massachusetts in 1997 and 1998, the Eugene M. Isenberg Award from the Isenberg School of Management, University of Massachusetts, in 1999 and 2000, and the Third Place 2016 Bell Labs Award. He was the General Chair of the 2011 IEEE RFID Technology and Applications Conference and the General Co-Chair of the 2011 IEEE MTT-S IMWS on Millimeter-Wave Integration Technologies. He was the Chairman of the EU COST Action IC0803 RF/Microwave Communication Subsystems for Emerging Wireless Technologies, and is currently the Vice-Chair of the EU COST Action IC1301 Wireless Power Transmission for Sustainable Electronics. He was the Coordinator of the Marie Curie Industry-Academia Pathways and Partnerships project Symbiotic Wireless Autonomous Powered system. He was an Associate Editor of the *IET Microwaves Antennas and Propagation Journal*, *IEEE MICROWAVE AND WIRELESS COMPONENTS LETTERS*, and the *IEEE RFID VIRTUAL JOURNAL*. He serves as an Associate Editor of the *IEEE JOURNAL ON RFID*. He is the Founder and the Editor-in-Chief of the *Cambridge Wireless Power Transfer Journal*. He is the Vice Chair of the URSI Commission D, Electronics and Photonics, and the ADCOM Member of the IEEE Council on RFID serving as the Vice President of Conferences. He is a Distinguished Lecturer of the IEEE Council on RFID.



Jimmy G. Hester (S'14) received the bachelor's and M.S. degrees in electrical and signal processing engineering (with a major in radio frequency electronics) from INP Toulouse, ENSEEIHT, Toulouse, France, in 2012 and 2014, respectively, and the M.S. degree in electrical and computer engineering from the Georgia Institute of Technology, Atlanta, GA, USA, in 2014, where he is currently pursuing the Ph.D. degree in electrical and computer engineering.

He spent two intense preparation years studying fundamental chemistry, math, and physics. He is currently a Research Assistant with the ATHENA Group, Georgia Institute of Technology. His current research interests include the interface between radio-frequency engineering and material science in the form of flexible electronics technologies and nanotechnologies, the use of carbon nanomaterials applied to inkjet-printed RF sensing components for flexible low-cost ubiquitous gas sensing applications and the development process, from the development of inkjet inks, improvement of fabrication methods, sensor component design, high-frequency characterization, environmental testing to the design, and simulation and fabrication of the RF system embedding the sensor.



Manos M. Tentzeris (S'89–M'92–SM'03–F'10) received the Diploma (*magna cum laude*) degree in electrical and computer engineering from the National Technical University of Athens, Athens, Greece, and the M.S. and Ph.D. degrees in electrical engineering and computer science from the University of Michigan, Ann Arbor, MI, USA.

He was a Visiting Professor with the Technical University of Munich, Munich, Germany, in 2002, a Visiting Professor with GTRI-Ireland, Athlone, Ireland, in 2009, and a Visiting Professor with LAAS-CNRS, Toulouse, France, in 2010. He has given more than 100 invited talks to various universities and companies all over the world. He has helped to develop academic programs in 3-D/inkjet-printed RF electronics and modules, flexible electronics, origami and morphing electromagnetics, highly integrated/multilayer packaging for RF and wireless applications using ceramic and organic flexible materials, paper-based RFIDs and sensors, wireless sensors and biosensors, wearable electronics, "Green" electronics, energy harvesting and wireless power transfer, nanotechnology applications in RF, microwave MEMS, and SOP-integrated (UWB, multiband, millimeter-wave, and conformal) antennas, and heads the ATHENA Research Group (20 researchers). He served as the Head of the GT-ECE Electromagnetics Technical Interest Group, the Georgia Electronic Design Center Associate Director of RFID/Sensors Research, the Georgia Tech NSF-Packaging Research Center Associate Director of RF Research, and the RF Alliance Leader with the Georgia Institute of Technology, Atlanta, GA, USA, where he is currently a Ken Byers Professor of flexible electronics with the School of Electrical and Computer Engineering. He has authored more than 620 papers in refereed journals and conference proceedings, 5 books, and 25 book chapters.

Dr. Tentzeris is a member of the URSI-Commission D, the MTT-15 Committee, and the Technical Chamber of Greece, and is an Associate Member of EuMA. He is a Fellow of the Electromagnetic Academy. He was a recipient/co-recipient of the 2016 Bell Labs Award Third Prize,

the 2015 IET Microwaves, Antennas and Propagation Premium Award, the 2014 Georgia Tech ECE Distinguished Faculty Achievement Award, the 2014 IEEE RFID-TA Best Student Paper Award, the 2013 IET Microwaves, Antennas and Propagation Premium Award, the 2012 FiDiPro Award in Finland, the iCMG Architecture Award of Excellence, the 2010 IEEE Antennas and Propagation Society Piergiorgio L. E. Uslenghi Letters Prize Paper Award, the 2011 International Workshop on Structural Health Monitoring Best Student Paper Award, the 2010 Georgia Tech Senior Faculty Outstanding Undergraduate Research Mentor Award, the 2009 IEEE TRANSACTIONS ON COMPONENTS AND PACKAGING TECHNOLOGIES Best Paper Award, the 2009 E. T. S. Walton Award from the Irish Science Foundation, the 2007 IEEE APS Symposium Best Student Paper Award, the 2007 IEEE IMS Third Best Student Paper Award, the 2007 ISAP 2007 Poster Presentation Award, the 2006 IEEE MTT Outstanding Young Engineer Award, the 2006 Asia-Pacific Microwave Conference Award, the 2004 IEEE TRANSACTIONS ON ADVANCED PACKAGING Commendable Paper Award, the 2003 NASA Godfrey "Art" Anzic Collaborative Distinguished Publication Award, the 2003 IBC International Educator of the Year Award, the 2003 IEEE CPMT Outstanding Young Engineer Award, the 2002 International Conference on Microwave and Millimeter-Wave Technology Best Paper Award (Beijing, China), the 2002 Georgia Tech-ECE Outstanding Junior Faculty Award, the 2001 ACES Conference Best Paper Award, the 2000 NSF CAREER Award, and the 1997 Best Paper Award of the International Hybrid Microelectronics and Packaging Society. He was a TPC Chair of the IEEE IMS 2008 Symposium and the Chair of the 2005 IEEE CEM-TD Workshop and is the Vice-Chair of the RF Technical Committee of the IEEE CPMT Society. He is the founder and the Chair of the RFID Technical Committee of the IEEE MTT Society and the Secretary/Treasurer of the IEEE C-RFID. He is an Associate Editor of the IEEE TRANSACTIONS ON MICROWAVE THEORY AND TECHNIQUES, the IEEE TRANSACTIONS ON ADVANCED PACKAGING, and the *International Journal on Antennas and Propagation*. He served as one of the IEEE MTT-S Distinguished Microwave Lecturers from 2010 to 2012 and is one of the IEEE CRFID Distinguished Lecturers.